

A Grid Cell Inspired Model of Cortical Column Function

Jochen Kerdels and Gabriele Peters

*FernUniversitt in Hagen – University of Hagen,
Human-Computer Interaction, Faculty of Mathematics and Computer Science,
Universitätsstrasse 1, D-58097 Hagen, Germany*

Keywords: Cortical Column, Autoassociative Memory, Grid Cells, Attractor Dynamics.

Abstract: The cortex of mammals has a distinct, low-level structure consisting of six horizontal layers that are vertically connected by local groups of about 80 to 100 neurons forming so-called minicolumns. A well-known and widely discussed hypothesis suggests that this regular structure may indicate that there could be a common computational principle that governs the diverse functions performed by the cortex. However, no generally accepted theory regarding such a common principle has been presented so far. In this position paper we provide a novel perspective on a possible function of cortical columns. Based on our previous efforts to model the behaviour of entorhinal grid cells we argue that a single cortical column can function as an independent, autoassociative memory cell (AMC) that utilizes a sparse distributed encoding. We demonstrate the basic operation of this AMC by a first set of preliminary simulation results.

1 INTRODUCTION

The mammalian cortex has a remarkably regular, low-level structure. It is organized into six horizontal layers, which are vertically connected by local groups of about 80 to 100 neurons (in primates) that form so-called *minicolumns*. These minicolumns are in turn connected by local, short-range horizontal connections forming cortical *macrocolumns* (sometimes referred to as just *columns* or *modules*) in a self-similar fashion (Mountcastle, 1978; Mountcastle, 1997; Buxhoeveden and Casanova, 2002). This general pattern of organization into layers and (mini)columns suggests that there might be a common computational principle that governs the diverse functions performed by the cortex. Theories regarding such a common principle cover a wide range of putative mechanisms and models including, among others, an updated version of the hierarchical temporal memory (HTM) model (Hawkins et al., 2017), which postulates that individual columns can learn predictive models of entire objects by combining sensory data with a location input that indicates the spatial origin of the respective data; a sparse distributed coding model (Rinkus, 2017) that relates the functions of macro- and minicolumns by postulating that minicolumns enforce the sparsity of a sparse distributed representation stored and recognized by individual macrocolumns; or a cortical column model based

on predictability minimization (Hashmi and Lipasti, 2009). Whether any of the existing hypothesis regarding the potential function of cortical columns pertains, or if there is any common computational principle at all remains controversial (Horton and Adams, 2005).

In this paper we approach the question whether the columnar structure of the cortex reflects a common computational principle by focusing on a putative core function of the cortical minicolumn that is implemented by a specific subset of neurons while leaving the overall function of the entire minicolumn unspecified for now. Given the canonical connectivity of cortical principal cells shown in figure 1, we argue that groups of layer 2/3 and upper layer 5 neurons (L2/3PC and L5ITN in Fig. 1) form a local, autoassociative memory that builds the core functionality of a minicolumn while all other neurons depicted in figure 1 serve supporting functions, e.g., communication to subcerebral targets (L5SPN), communication to long-range cortical targets (L6CC), modulation of sensory input or input from lower-order cortex (L6CT), or modulation of the autoassociative memory itself (L4PC). We base this hypothesis on earlier work directed at modeling and understanding of *grid cells* located in layer 2/3 and layer 5 of the medial entorhinal cortex (Fyhn et al., 2004; Hafting et al., 2005). While grid cells are commonly viewed as part of a specialized system for navigation and orientation (Ro-

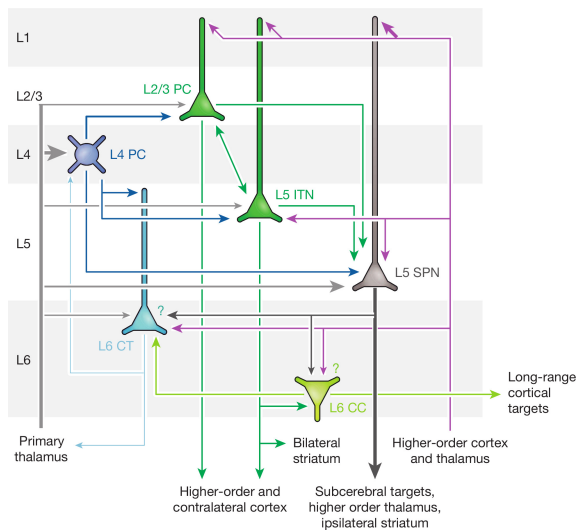


Figure 1: Canonical connectivity of cortical principal cells. Reprinted with permission from (Harris and Mrsic-Flogel, 2013). PC: principal cell, ITN: intratelencephalic neuron, SPN: subcerebral projection neuron, CT: corticothalamic neuron, CC: corticocortical neuron. Line thickness represents the strength of a pathway, question marks indicate connections that appear likely but have not yet been directly shown.

wland et al., 2016), it can be demonstrated that their behavior can also be interpreted as just one instance of a more general information processing scheme (Kerdels and Peters, 2015; Kerdels, 2016). Here we extend this idea by generalizing and augmenting the previous grid cell model into an autoassociative memory model describing the core function of a cortical minicolumn.

The next section revisits the grid cell model (GCM) upon which the proposed autoassociative memory model will be built. At its core the GCM is based on the recursive growing neural gas (RGNG) algorithm, which will also be a central component of the new model. Section 3 introduces a first set of changes to the original GCM on the individual neuron level that improve the long-term stability of learned representations, and allow the differentiation between processes occurring in the proximal and distal sections of the neuron's dendritic tree. In section 4 these changes are then integrated into a full autoassociative memory model, which consists of two distinct groups of neurons that interact reciprocally. Section 5 presents preliminary results of early simulations that support the basic assumptions of the presented model. Finally, section 6 discusses the prospects of the proposed perspective on cortical minicolumns and outlines our future research agenda in that regard.

2 RGNG-BASED GRID CELL MODEL

Grid cells are neurons in the entorhinal cortex of the mammalian brain whose individual activity correlates strongly with periodic patterns of physical locations in the animal's environment (Fyhn et al., 2004; Hafting et al., 2005; Rowland et al., 2016). This property of grid cells makes them particularly suitable for experimental investigation and provides a rare view into the behavior of cortical neurons in a higher-order part of the brain. The most prevalent view on grid cells so far interprets their behavior as part of a specialized system for navigation and orientation (Rowland et al., 2016). However, from a more general perspective the activity of grid cells can also be interpreted in terms of a domain-independent, general information processing scheme as shown by the RGNG-based GCM of Kerdels and Peters (Kerdels and Peters, 2015; Kerdels, 2016). The main structure of this model can be summarized as follows: Each neuron is viewed as part of a local group of neurons that share the same set of inputs. Within this group the neurons compete against each other to maximize their activity while trying to inhibit their peers. In order to do so, each neuron tries to learn a representation of its *entire* input space by means of competitive Hebbian learning. In this process the neuron learns to recognize a limited number of prototypical input patterns that optimally originate from maximally diverse regions of the input space. This learned set of input pattern prototypes then constitutes the sparse, pointwise input space representation of the neuron. On the neuron group level the competition among the neurons forces the individual, sparse input space representations to be pairwise distinct from one another such that the neuron group as a whole learns a joint input space representation that enables the neuron group to work as a *sparse distributed memory* (Kanerva, 1988).

The GCM uses the recursive growing neural gas algorithm (RGNG) to simultaneously describe both the learning of input pattern prototypes on the level of individual neurons as well as the competition between neurons on the neuron group level. In contrast to the common notion of modeling neurons as simple integrate and fire units, the RGNG-based GCM assumes that the complex dendritic tree of neurons possesses more computational capabilities. More specifically, it assumes that individual subsections of a neuron's dendritic tree can learn to independently recognize different input patterns. Recent direct observations of dendritic activity in cortical neurons suggest that this assumption appears biologically plausible (Jia et al., 2010; Chen et al., 2013). In the model

this intra-dendritic learning process is described by a single growing neural gas per neuron, i.e., it is assumed that some form of competitive Hebbian learning takes place within the dendritic tree. Similarly, it is assumed that the competition between neurons on the neuron group level is Hebbian in nature as well, and is therefore modeled by analogous GNG dynamics. For a full formal description and an in-depth characterization of the RGNG-based GCM we refer to (Kerdels and Peters, 2016; Kerdels, 2016). In the following section we focus on describing our modifications to the original RGNG-based GCM.

3 EXTENDED NEURON MODEL

Although the neuron model outlined in the previous section was conceived to describe the activity of entorhinal grid cells, it can already be understood as a general computational model of certain cortical neurons, i.e., L2/3 PC and L5 ITN in figure 1. However, to function as part of our cortical column model we modified the existing GCM with respect to a number of aspects:

3.1 Ensemble Activity

In response to an input ξ the GCM returns an ensemble activity vector \mathbf{a} where each entry of \mathbf{a} corresponds to the activity of a single neuron. Given a neuron group of N neurons, the ensemble activity \mathbf{a} is calculated as follows: For each neuron $n \in N$ the two prototypical input patterns \mathbf{s}_1^n and \mathbf{s}_2^n that are closest to input ξ are determined among all prototypical input patterns I^n learned by the dendritic tree of neuron n , i.e.,

$$\begin{aligned} \mathbf{s}_1^n &:= \arg \min_{\mathbf{v} \in I^n} \|\mathbf{v} - \xi\|_2 \\ \mathbf{s}_2^n &:= \arg \min_{\mathbf{v} \in I^n \setminus \{\mathbf{s}_1^n\}} \|\mathbf{v} - \xi\|_2. \end{aligned}$$

The ensemble activity $\mathbf{a} := (a_0, \dots, a_{N-1})$ of the group of neurons is then given by

$$a_i := 1 - \frac{\|\mathbf{s}_1^i - \xi\|_2}{\|\mathbf{s}_2^i - \xi\|_2}, \quad i \in \{0, \dots, N-1\}, \quad (1)$$

followed by a softmax operation on \mathbf{a} . Thus, the activity of each neuron is determined by the relative distances between the current input and the two best matching prototypical input patterns. If the input is about equally distant to both prototypical input patterns the activity is close to zero, and if the input is much closer to the best pattern than the second best pattern the activity approaches one. The competition among the neurons on the group level ensures that for any given

input only a small, but highly specific (Kerdels and Peters, 2017) subset of neurons will exhibit a high activation resulting in a sparse, distributed encoding of the particular input.

Compared to the original GCM (Kerdels and Peters, 2016; Kerdels, 2016) we modified the activation function (Eq. 1) to allow for a smoother response to inputs that are further away from the best matching unit s_1 than the distance between s_1 and s_2 , and we normalized the ensemble output using the softmax operation.

3.2 Learning Rate Adaptation

The original GCM uses fixed learning rates ϵ_b and ϵ_n , which require to find a tradeoff between learning rates that are high enough to allow for a reliable adaptation and alignment of initially random prototypes and learning rates that are low enough to ensure a relatively stable long-term representation of the respective input space. We modified the original GCM in that regard by introducing three learning phases that shape the learning rates used by the GCM. During the initial learning phase both ϵ_b and ϵ_n are kept at their initial values (e.g., $\epsilon_b = \epsilon_n = 0.01$). The duration t_1 (measured in # of inputs) of this first phase depends on the maximum number of prototypes M and the interval λ with which new prototypes are added to the model¹, i.e., $t_1 = 2M\lambda$. This duration ensures that the RGNG underlying the GCM has enough time to grow to its maximum size and to find an initial alignment of its prototypes. The second learning phase is a short transitional phase with a duration $t_2 = M\lambda$ in which both learning rates ϵ_b and ϵ_n are reduced by one order of magnitude to allow the initial alignment to settle in a more stable configuration. Up to this point the prototypes learned by the individual neurons of the model are likely to be similar as primary learning rate ϵ_b and secondary learning rate ϵ_n are equal so far². Beginning with the last learning phase, which is open-ended in its duration, only the secondary learning rate ϵ_n is reduced once more by two orders of magnitude. This asymmetric reduction of ϵ_n initiates a differentiation process among the individual neurons that allows the prototypes of each neuron to settle on distinct locations of the input space.

¹Both M and λ are parameters of the RGNG used by the original GCM.

²See (Kerdels, 2016) for details on how primary and secondary learning rates relate within an RGNG.

3.3 Handling of Repetitive Inputs

Since the GCM is a continuously learning model it has to be able to cope with repetitive inputs in such a way that its learned representation is not distorted if it is exposed to a single repeated input. Without adaptation a repeated input would correspond to an artificial increase in learning rate. To handle such a situation we adjust the learning rates ϵ_b and ϵ_n by an attenuation factor ζ :

$$\zeta = 0.1^{|s_1|/10},$$

with $|s_1|$ the number of successive times prototype s_1 was the best matching unit. The attenuation factor ζ is applied when $|s_1| > 1$.

3.4 Integration of Feedback Input

In order to use the GCM as part of our cortical column model, we modified the existing GCM to allow the integration of feedback connections. In the cortex such feedback connections originate from higher-order regions (violet arrows in Fig. 1) and predominantly terminate in layer 1 on the distal dendrites of layer 2/3 and layer 5 neurons. To integrate these feedback connections into the model we added a secondary GNG to the description of each neuron. With this extension the dendritic tree of each neuron is now modeled by two GNGs: a primary GNG that represents the proximal dendrites that process the main inputs to the neuron, and a secondary GNG that represents the distal dendrites that process feedback inputs. Both GNGs can independently elicit the neuron to become active when either GNG receives a matching input. If both GNGs receive inputs simultaneously, the output o_p of the primary GNG (determined by the ratio shown in Eq. 1) is modulated by the output o_s of the secondary GNG depending on the *agreement* between outputs o_p and o_s :

$$a^* := \frac{1}{1 + e^{-(o_p - \phi)(1 + \gamma(1 - |o_p - o_s|))}},$$

with parameter γ determining the strength of the modulation and parameter ϕ determining at which activity level (Eq. 1) of o_p the output is increased or decreased, respectively. Typical values are, e.g., $\gamma = 10$ and $\phi = 0.5$.

A second important relation between the primary and the secondary GNG concerns learning of new prototypical input patterns. The secondary GNG can only learn when the primary GNG has received a matching input that resulted in an activation of the neuron, i.e., the learning rates ϵ_b and ϵ_n of the secondary

GNG are scaled by the output of the primary GNG in response to a current main input to the neuron:

$$\begin{aligned} \epsilon_b^* &:= \epsilon_b o_p, \\ \epsilon_n^* &:= \epsilon_n o_p, \end{aligned}$$

or by zero if there is no main input present. As a consequence, the secondary GNG learns to represent only those parts of the feedback input space that correlate with regions of the main input space that are directly represented by the prototypical input patterns of the primary GNG. This way, the secondary GNG learns to respond only to those feedback signals that regularly co-occur with those main input patterns that were learned by the primary GNG. One possible neurobiological mechanism that could establish such a relation between proximal and distal dendrites is the back-propagation of action potentials (Stuart et al., 1997; Waters et al., 2005).

Together, the primary and secondary GNG allow a modeled neuron to learn a representation of its main input space while selectively associating feedback information that may help to disambiguate noisy or distorted main input or substitute such input if it is missing.

4 CORTICAL COLUMN MODEL

So far the extended neuron model describes a single group of neurons that is able to learn a sparse, distributed representation of its input space and is able to integrate additional feedback input. As such, the group acts as a local, input-driven transformation that maps input signals to output signals without maintaining an active state, i.e., if no input is present, no output will be generated. However, if two groups share the same main input space but also receive the group activity of each other as an additional input signal, both groups would be able to maintain a stable active state even when the main input signal vanishes. Instead of being stateless input-output transformations the two groups would form an *active autoassociative memory cell* (AMC) (Kanerva, 1988; Kanerva, 1992). Given the canonical connectivity of cortical principal cells shown in figure 1 we argue that L2/3PC and L5ITN constitute such a pair of reciprocally connected neuron groups forming an AMC. Both groups share a main input space via connections from the primary thalamus and local L4PC, while they also both receive feedback input at their distal dendrites in layer 1 from higher-order cortex and the thalamus³.

³These feedback connections motivated the extension described in section 3.4.

The other neuron groups shown in figure 1 can be interpreted as providing support for the AMC: The outputs of both L2/3PC and L5ITN connect locally to L5SPN, which projects to subcerebral targets, e.g., motor centres, and non-locally to higher-order parts of the cortex. The output of the lower group L5ITN makes an additional local connection to L6CC, which projects to long-range cortical targets, but also locally to L6CT, which in turn connects back to L4PC and the primary thalamus.

We propose that the described neural structure constitutes a single cortical minicolumn. At its core the minicolumn hosts a single autoassociative memory cell (L2/3PC / L5ITN) that is supported by neurons regulating its activity (L4PC), its input (L4PC / L6CT) and its output (L5SPN / L6CC).

A key property of the described AMC is its ability to feed its output back into itself via the reciprocal connections between the two neuron groups (L2/3PC / L5ITN). This local feedback loop does not only allow the AMC to stay active when the main input vanishes. It also enables a form of attractor dynamics (Kanerva, 1988; Kanerva, 1992) where an initial, potentially noisy or ambiguous input pattern can be iteratively refined to approach one of the stable, prototypical input patterns learned by the AMC. In addition, this iterative process can be supported or modulated by the feedback input integrated via the distal dendrites of both neuron groups. On a cortex-wide level these attractor dynamics might play an important role to dynamically bind subsets of cortical minicolumns into joint, temporarily stable attractor states.

5 PRELIMINARY RESULTS

As a first step towards implementing the cortical column model outlined in the previous section we simulated a single AMC consisting of two neuron groups a and b , which correspond to the two neuron groups L2/3PC and L5ITN of figure 1. Each neuron group was modeled by the extended GCM described in section 3 containing 25 neurons with 16 dendritic prototypes each. Further parameters are given in table 1. As input both groups received samples from the MNIST database of handwritten digits (Lecun et al., 1998) reduced to a resolution of 16×16 pixels concatenated with the current ensemble activity of the other group. Each MNIST input was repeated $10 \times$ in a row combined in each case with the updated ensemble activity of the respective other neuron group allowing for the co-occurrence of the original input with the other group's reaction to that input. In total, the simulated AMC was presented with 20 million inputs corresponding

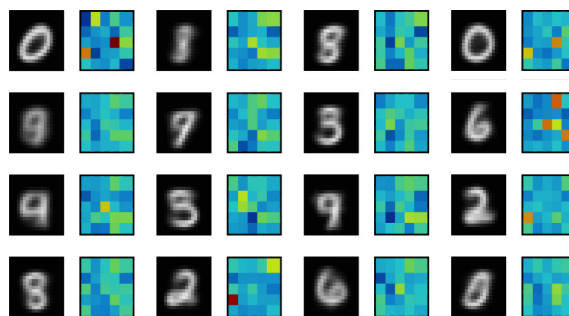


Figure 2: Sixteen prototypes learned by a *single* neuron of neuron group a . Each prototype consists of a 16×16 representation corresponding to the MNIST part of the input (shown in gray) and a 5×5 representation corresponding to the group b ensemble activation part of the input (visualized as color gradient from blue (low activation) to red (high activation)).

to about 33 full presentations of the MNIST training data set to the system.

Figure 2 shows the 16 dendritic prototypes learned by a *single* neuron of group a after a total of 20 million inputs. Like the input patterns the prototypes consist of two parts: a 16×16 representation corresponding to the MNIST portion of the input and a 5×5 representation corresponding to the ensemble activation of neuron group b co-occurring with the particular MNIST inputs. The MNIST part of the prototypes indicate that the neuron is, as expected, learning a sparse, pointwise representation of its entire input space. While some prototypes exhibit clear and distinct shapes that indicate that these prototypes have already settled at stable locations in input space, a few prototypes have less distinct shapes indicating that these prototypes have not yet reached such stable locations. One important aspect to note is that this neuron will exhibit a high activity for *any* of the learned input patterns. As a consequence, looking just at the activity of this individual neuron it is not possible to tell whether the input was a, e.g., “0” or “2” or any of the other patterns represented by one of the neuron’s prototypes.

A disambiguation of the input becomes only possible when observing the ensemble activity of an entire neuron group, i.e., the representation of the input is distributed across the entire group. No individual neuron encodes for just a single input. Such ensemble activities are captured by the ensemble part of the prototypes and show, in this case, the average ensemble activity of group b in response to the respective MNIST input captured by the MNIST part of the prototypes. The ensemble activities of group b shown in figure 2 show that each input pattern evokes a distinct pattern of ensemble activity allowing to disambiguate the different input patterns. In case of already stable

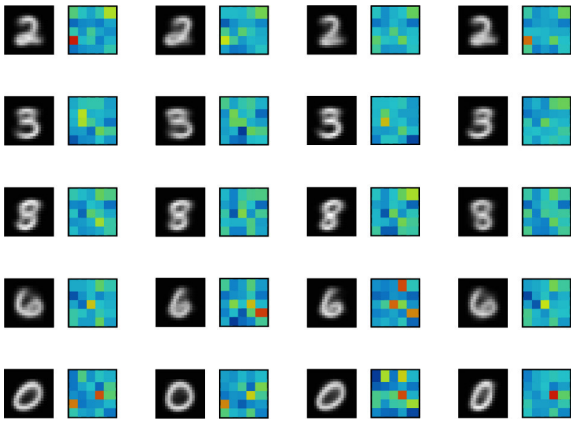


Figure 3: Twenty examples of learned prototypes from different neurons of group a that represent numbers of similar shape. Visualization as in Fig. 2.

prototypes it can also be seen, that the ensemble activity tends to be sparse with only a few neurons exhibiting a strong activation in response to a particular input.

One interesting question regarding such a sparse, distributed representation is the degree of variation in this ensemble code if very similar inputs are processed. Figure 3 shows twenty examples of dendritic prototypes from different neurons of group a that represent numbers of similar shape. The captured ensemble activities of group b indicate that the similarity of activation patterns appears to match well with the similarity of the corresponding MNIST patterns. Even in cases with an overall low activation like the responses to the number “8” (third row), the corresponding ensemble codes appear similar.

These first tentative results indicate, that the proposed model appears to be able to learn a sparse, distributed representation of its main input space (here the MNIST set), while simultaneously learning the ensemble codes of an accompanying group of neurons that operates on the same input space.

6 CONCLUSION

The cortical column model outlined in this paper is still in a very early stage. Yet, it combines multiple, novel ideas that will guide our future research. First, the RGNG-based, unsupervised learning of a sparse, distributed input space representation utilizes a classic approach of prototype-based learning in a novel way. Instead of establishing a one-to-one relation between a learned representation (prototype) and a corresponding region of input space, it learns an ensemble code that utilizes the response of multiple neurons

(sets of prototypes) to a given input. The presented preliminary results indicate that learning such an ensemble code appears feasible. Our future research in this regard will focus on improving our understanding of the resulting ensemble code, as well as improving the RGNG algorithm in terms of learning speed and robustness w.r.t. a continuous learning regime.

Second, the idea of reciprocally connecting two neuron groups that process a shared input space enables the creation of an *autoassociative memory cell* (AMC) that is able to maintain an active state even in the absence of any input. In addition, such an AMC may exhibit some form of attractor dynamics where the activities of the two, reciprocally connected neuron groups self-stabilize. A precondition for such an AMC is the groups’ ability to learn the ensemble code of the respective other group. The presented preliminary results indicate that this is possible. Our future research will focus on understanding the characteristics of the dynamics of such an AMC, e.g., in response to various kinds of input disturbances.

Third, the outlined cortical column model suggests that the cortex may consist of a network of autoassociative memory cells that influence each other via feedback as well as feedforward connections while trying to achieve locally stable attractor states. In addition, further cortical circuitry may modulate the activity of individual cortical columns to facilitate competition among cortical columns or groups of cortical columns on a more global level, which may then lead to the emergence of stable, global attractor states that are able to temporarily bind together sets of cortical columns. In this context our research is still in its infancy and will focus on implementing a first version of a full cortical column model that can then be tested in small hierarchical network configurations, e.g., to process more complex visual input.

REFERENCES

- Buxhoeveden, D. P. and Casanova, M. F. (2002). The minicolumn hypothesis in neuroscience. *Brain*, 125(5):935–951.
- Chen, T.-W., Wardill, T. J., Sun, Y., Pulver, S. R., Renninger, S. L., Baohan, A., Schreier, E. R., Kerr, R. A., Orger, M. B., Jayaraman, V., Looger, L. L., Svoboda, K., and Kim, D. S. (2013). Ultrasensitive fluorescent proteins for imaging neuronal activity. *Nature*, 499(7458):295–300.
- Fyhn, M., Molden, S., Witter, M. P., Moser, E. I., and Moser, M.-B. (2004). Spatial representation in the entorhinal cortex. *Science*, 305(5688):1258–1264.
- Hafting, T., Fyhn, M., Molden, S., Moser, M.-B., and Moser, E. I. (2005). Microstructure of a spatial map in the entorhinal cortex. *Nature*, 436(7052):801–806.

Harris, K. D. and Mrsic-Flogel, T. D. (2013). Cortical connectivity and sensory coding. *Nature*, 503:51.

Hashmi, A. G. and Lipasti, M. H. (2009). Cortical columns: Building blocks for intelligent systems. In *2009 IEEE Symposium on Computational Intelligence for Multimedia Signal and Vision Processing*, pages 21–28.

Hawkins, J., Ahmad, S., and Cui, Y. (2017). Why does the neocortex have columns, a theory of learning the structure of the world. *bioRxiv*.

Horton, J. C. and Adams, D. L. (2005). The cortical column: a structure without a function. *Philosophical Transactions of the Royal Society of London B: Biological Sciences*, 360(1456):837–862.

Jia, H., Rochefort, N. L., Chen, X., and Konnerth, A. (2010). Dendritic organization of sensory input to cortical neurons in vivo. *Nature*, 464(7293):1307–1312.

Kanerva, P. (1988). *Sparse Distributed Memory*. MIT Press, Cambridge, MA, USA.

Kanerva, P. (1992). *Sparse distributed memory and related models [microform] / Pentti Kanerva*. Research Institute for Advanced Computer Science, NASA Ames Research Center.

Kerdels, J. (2016). *A Computational Model of Grid Cells based on a Recursive Growing Neural Gas*. PhD thesis, FernUniversität in Hagen.

Kerdels, J. and Peters, G. (2015). A new view on grid cells beyond the cognitive map hypothesis. In *8th Conference on Artificial General Intelligence (AGI 2015)*.

Kerdels, J. and Peters, G. (2016). Modelling the grid-like encoding of visual space in primates. In *Proceedings of the 8th International Joint Conference on Computational Intelligence, IJCCI 2016, Volume 3: NCTA, Porto, Portugal, November 9-11, 2016.*, pages 42–49.

Kerdels, J. and Peters, G. (2017). Entorhinal grid cells may facilitate pattern separation in the hippocampus. In *Proceedings of the 9th International Joint Conference on Computational Intelligence, IJCCI 2017, Funchal, Madeira, Portugal, November 1-3, 2017.*, pages 141–148.

Lecun, Y., Bottou, L., Bengio, Y., and Haffner, P. (1998). Gradient-based learning applied to document recognition. *Proceedings of the IEEE*, 86(11):2278–2324.

Mountcastle, V. B. (1978). An organizing principle for cerebral function: The unit model and the distributed system. In Edelman, G. M. and Mountcastle, V. V., editors, *The Mindful Brain*, pages 7–50. MIT Press, Cambridge, MA.

Mountcastle, V. B. (1997). The columnar organization of the neocortex. *Brain*, 120(4):701–722.

Rinkus, G. J. (2017). A cortical sparse distributed coding model linking mini- and macrocolumn-scale functionality. *ArXiv e-prints*.

Rowland, D. C., Roudi, Y., Moser, M.-B., and Moser, E. I. (2016). Ten years of grid cells. *Annual Review of Neuroscience*, 39(1):19–40. PMID: 27023731.

Stuart, G., Spruston, N., Sakmann, B., and Husser, M. (1997). Action potential initiation and backpropagation in neurons of the mammalian CNS. *Trends in Neurosciences*, 20(3):125 – 131.

Waters, J., Schaefer, A., and Sakmann, B. (2005). Back-propagating action potentials in neurones: measurement, mechanisms and potential functions. *Progress in Biophysics and Molecular Biology*, 87(1):145 – 170. Biophysics of Excitable Tissues.

APPENDIX

Parameterization

The neuron groups modeled by the extended GCM described in section 3 use an underlying, two-layered RGNG. Each layer of an RGNG requires its own set of parameters. In this case we use the sets of parameters θ_1 and θ_2 , respectively. Parameter set θ_1 controls the inter-neuron level of the GCM while parameter set θ_2 controls the intra-neuron level. Table 1 summarizes the parameter values used for the simulation runs presented in this paper. For a detailed characterization of these parameters we refer to (Kerdels, 2016).

Table 1: Parameters of the RGNG-based, extended GCM used for the preliminary results presented in section 5. For a detailed characterization of these parameters we refer to the appendix and (Kerdels, 2016).

θ_1	θ_2
$\epsilon_b = 0.04$	$\epsilon_b = 0.01$
$\epsilon_n = 0.04$	$\epsilon_n = 0.01$
$\epsilon_r = 0.01$	$\epsilon_r = 0.01$
$\lambda = 1000$	$\lambda = 1000$
$\tau = 100$	$\tau = 100$
$\alpha = 0.5$	$\alpha = 0.5$
$\beta = 0.0005$	$\beta = 0.0005$
$M = 25$	$M = 16$